Numerical Simulation of the Impact of Diaphragm Wall Construction on Adjacent Tunnels

Shimin Zhang[1], Yang Lyu[1*], Tonghua Wang[2], Guiying Huang[1], Jinhong Zhang[3]

[1.] School of Engineering, Hangzhou City University, Hangzhou 310015, China
[2.] Beijing Urban Construction Design & Development Group Co.,Ltd, Beijing 100037, China
[3.] Zhejiang Provincial Architectural Design & Research Institute Co.,Ltd, Hangzhou 310006, China

*Correspondence: Yang Lyu (2230302011@stu.hzcu.edu.cn)

Abstract. To investigate the impact of diaphragm wall construction on adjacent tunnels, numerical simulations were conducted using Plaxis 3D finite element software based on relevant engineering cases. A bilinear model was employed to simulate the trench wall pressure, and two different constitutive models were applied to analyze the influence of diaphragm wall construction on the horizontal displacement and settlement of the tunnel. The effects of various construction factors, such as the distance between the tunnel and the diaphragm wall, the excavation depth of the diaphragm wall, and the trench excavation method, were quantified. The results indicate that the horizontal and vertical displacements of the tunnel are most significant during the concrete pouring stage, and the horizontal deformation data closely follow a Gaussian distribution. The horizontal and vertical displacements of the tunnel are positively correlated with the depth of the diaphragm wall and negatively correlated with the horizontal distance between the tunnel and the diaphragm wall. Furthermore, the segmented excavation method can reduce the impact on adjacent tunnels. The findings provide theoretical references and numerical methods for evaluating the influence of diaphragm wall construction on the deformation of adjacent subway tunnels.

Keywords: Diaphragm wall; Tunnel deformation; Numerical simulation; Gaussian distribution; Construction factors

1 Introduction

Metro system, the mainframe of urban transport system has an important part to play to take down the amount of vehicles stuck up there, and also making our living space more prosperous. But foundation pit construction near to metro tunnels changed soil's pressure status around it and gave many difficult consequences for the existing tunnels structures[1-5]. And then research shows like it was like huge tunnel movements when we would construct things under things which would make up more than 43.81% according to other research[6] of everything that moved during this period. These sorts of displacements could threaten tunnel integrity and running safety; hence we should carry

© The Author(s) 2026
S. Sing et al. (eds.), *Proceedings of the 2025 7th International Conference on Civil Architecture and Urban Engineering (ICCAUE 2025)*, Atlantis Highlights in Engineering 43,
https://doi.org/10.2991/978-94-6239-682-1_24

out further investigation into the effect of D-wall construction upon the neighboring metro tunnels.

The current work takes on theoretical, numerical, field monitoring, and model testing ways of looking at how tunnels react when you dig big holes around them. Such as Wang et al[7] and Zhang et al[8], they use Boussinesq's Elastic Solution to study the additional stress effect. Yin [9] utilized HSS in ZSOIL to do research on D-wall design parameters. Wei [10] derived an empirical model of tunnel uplift based on 14 case histories, while Chen et al[11, 12] used centrifuge tests with numerical simulations. Also there are studies done about ground change caused by installing d-wall. report ground settlements ranging from 0.075% to 0.15% of excavation depth[13], and Dong[14] look at horizontal soil displacements and parameters sensitivity.

Previous studies on excavaiton-indued tunnel effectsand D-wall–induced ground movements, but no study on D-wall's stages influence on adjectnt tunnnels' displacement. The present investigation takes place regarding the influences on tunnels that arise out of building d-walls in the soil around shanghai via some numbers based tests made on different types. By looking at how the horizintal and vertical tunneledisplacements behave, all of those main parts in construction can have an evaluation based on them as it serves as a theory when it comes time to do risk assessments of building old tubes with things like this being done nearby.

2 Numerical Simulation

2.1 Project Overview

Project in Gongshu District,Hangzhou City is southwest of Dongxin & Shaoxing road and also near Metro Line 1 Tieguan station. South side is next to the tieguan station of metro line 1 and the tunnel part between the tieguan and zhalongkou station as well as the connecting line for intercity trains. And the boundary lines of our foundation pits for this support are about 9. 6 meters from the major structure of tieguan station when they're closest together. Support method uses 800mm wide diaphragm wall on all 4 sides, bottom end of the wall penetrates to gravel layer. The project overview map and geological profile are shown in Fig 1 and 2, respectively.

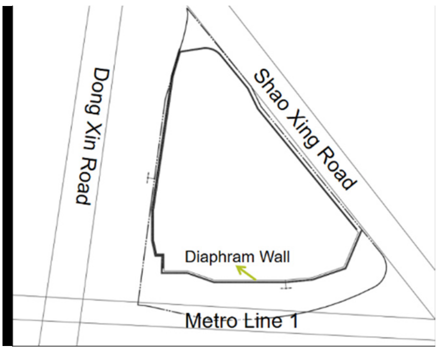

Fig. 1. Project Overview

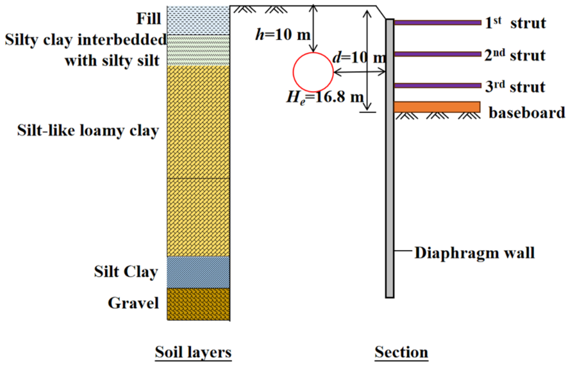

Fig. 2. Geological Profile

2.2 Calculation Model and Parameters

The HS-Small constitutive model, developed within the framework of the classical HS theory by Benz[15] , is an improved constitutive model. Its characteristics include comprehensively reflecting the unloading and small-strain behavior of soils, while considering the pressure-hardening and dilatancy of soft clay, and distinguishing between loading and unloading stiffness. These features make the HS-Small model particularly advantageous for simulating complex engineering problems such as deep foundation pit excavation[16-18]. Therefore, this study adopts the HS-Small model and utilizes Plaxis 3D finite element software for analysis. The finite element model is shown in Figures 3 and 4. The calculation trench panel is 6 m wide, 0.8 m thick, and 47 m deep. The tunnel is 50 m long with a radius of 3.1 m, and the trench panel is 10 m away from the tunnel. Considering boundary effects, the calculation model dimensions are set to 50 m long, 25 m wide, and 20 m high. The parameters for the HS-Small constitutive model are listed in Table 1. The tunnel is simulated using plate elements, assumed to be an elastic material with a thickness of 0.4 m, an elastic modulus of 3.45×10^4MPa, and a Poisson's ratio of 0.2. The groundwater level at the diaphragm wall construction site is set at 2 m below the ground surface. Groundwater seepage effects are not considered in the calculations.

Table 1. HSS Model Parameters Table

Soil layers	Fill	Silty clay interbedded with silty silt	Silt-like loamy clay	Silt Clay
Effective Cohesion c'/kPa	6.8	10.8	20.1	16.8
Effective Friction /(°)	29	29.8	28.7	28.6
Tangent Modulus E^{ref}_{oed} /MPa	2.6	3.9	3.1	3.3
Secant Modulus E^{ref}_{50} /MPa	4.38	6.83	3.44	4.66
Unloading/Reloading Modulus E^{ref}_{ur} /MPa	22.5	23.2	15.9	22.9

Failure Ratio R_f	0.78	0.89	0.85	0.93
Shear Strain $\gamma_{0.7}(10^{-4})$	2.9	3.6	4.2	3.7
Initial Shear Modulus $G^{ref}{}_0$ /MPa	23.8	168.46	73.19	128.98

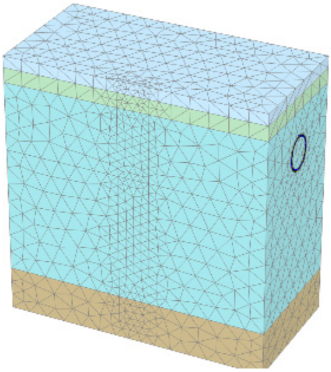

Fig. 3. Mesh Diagram

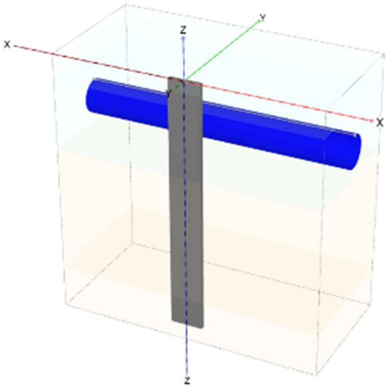

Fig. 4. Structural Diagram

2.3 Calculation Steps

The calculating model deals with all parts of the making process for the diaphragm walls; it looks at the stresses during four main stages: first is when there's no changing at all yet (that's the beginning of the stress), next up we start digging holes filled with special mix that stops it being too wet or dry before adding new concrete to it as soon as possible after the digging is finished. Model construction following these calculations procedure below:

Step 1: Initial equilibrium stress field. Tunnel is simulated by Plate element and it will be constructed first before excavation starts. Initial soil's own weight's stress area is calculated. For sake of calculation result being correct. In order to do so, right after having done the very initial stress computation, we reinitialize our calculation's resulting Displacements to zero value, yet preserving the already found out Stress-Fields outcome data into our future construction stages' simulation baseline starting points.

Step 2: The Trench Excavation and Slurry support are null elements which represent the part of the soil that is being excavated. Simultaneously Static Slurry Pressure (γ_b=12kN/m^3) is applied onto the trench wall and its base. Lateral pressure on trench walls from equation(1):

$$p = \gamma_b h \tag{1}$$

Step 3: Fluid Concrete Pouring: As it was researched in the existing, there have not yet become established standards with regard to how distribution should be for the pressure of the fluidic concrete. Therefore this paper chooses the theoretical model which has been given out by Lingset al. as an analysis framework.[19] Lateral pressure on trenches walls through bilinear model from eq(2) is calculated:

$$\begin{aligned} p &= \gamma_c z & z &\le h_{cr1} \\ p &= \gamma_c z + (\gamma_c - \gamma_b)\ h_{cr1} & z &> h_{cr1} \end{aligned} \tag{2}$$

where h_{cr1} is the critical depth of concrete, taken as 1/3 of the trench depth, and γ_c is the unit weight of concrete, 24 kN/m^3.

Step 4: Concrete Hardening. The null elements representing the excavated trench section are set as elastic elements. Simultaneously, the concrete pressure acting on the trench walls and base is removed to simulate concrete hardening.

3 Calculation Results and Analysis

The horizontal and vertical displacements of the tunnel at each stage obtained from the numerical simulation are shown as hollow scatter points in Figures 5 and 6. The maximum displacement of the tunnel occurs near the wall, gradually decreasing with distance from the wall. From the results of maximum displacement and change per stage shown in Figures 7 and 8, it can be observed that as the construction steps proceed, tunnel displacements initially increase and then decrease. During the trench excavation stage (Step 2), tunnel displacements are relatively small, with horizontal displacements ranging from approximately -0.05 to 0.7 mm and vertical displacements from 0.2 to 0.8 mm. The maximum values for both horizontal and vertical displacements occur during the concrete pouring stage (Step 3), with a maximum horizontal displacement of 2.10 mm and a maximum vertical displacement of 2.16 mm. During the concrete hardening stage (Step 4), tunnel displacements recover somewhat compared to the previous stage.

The change in horizontal displacement is relatively small, decreasing by about 2.4%, while the change in vertical displacement is larger, decreasing by about 4.9%.

To systematically analyze the displacement patterns of the tunnel induced by diaphragm wall construction, Gaussian functions were fitted to both horizontal and vertical displacement data for each construction stage. As shown in Figures 5 and 6, the fitted curves from Steps 2 to 4 exhibit high accuracy, with coefficients of determination (R^2) exceeding 0.99 for both displacement components, indicating negligible fitting error. The consistently high R^2 values—particularly notable in critical phases such as concrete pouring (Step 3)—confirm that the Gaussian distribution reliably captures the spatial variation of tunnel displacements throughout all construction stages, underscoring the statistical validity of the observed displacement patterns.

The numerical results indicate that the concrete pouring stage causes the most substantial tunnel displacements. This is due to the abrupt replacement of supporting slurry with fluid concrete, which changes the surrounding soil stress state and redistributes stress toward the tunnel. The observed near Gaussian displacement distribution along the tunnel axis agrees with the theory of spatial decay of construction induced disturbances, where effects weaken with distance from the source.

Additionally, a comparative analysis using the Mohr–Coulomb model was conducted. As shown in Figure 9, both constitutive models exhibit similar horizontal displacement trends, though the Mohr–Coulomb model yields slightly larger horizontal and vertical displacements than the HSS model. Figure 10 further indicates pronounced heave under the Mohr–Coulomb model, attributed to its inability to distinguish between loading and unloading responses, resulting in exaggerated stress release and soil uplift during excavation—a finding consistent with Ge and Zhou[20]. Thus, the HSS model provides more reasonable predictions in complex geotechnical conditions.

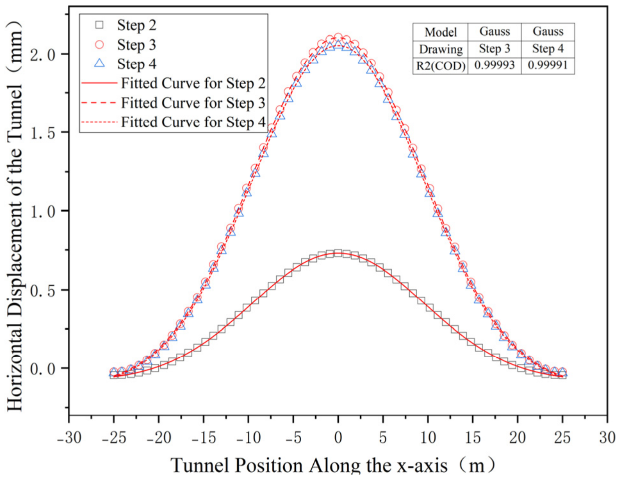

Fig. 5. HSS Model: Tunnel Horizontal Displacement and Fitting at Each Stage

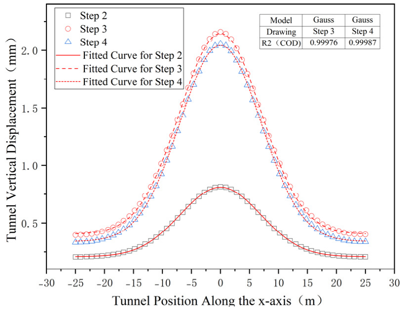

Fig. 6. HSS Model: Tunnel Vertical Displacement and Fitting at Each Stage

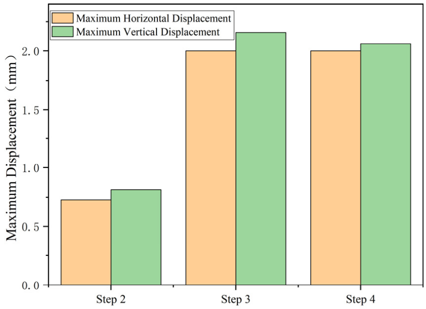

Fig. 7. HSS Model: Maximum Tunnel Displacement at Each Stage

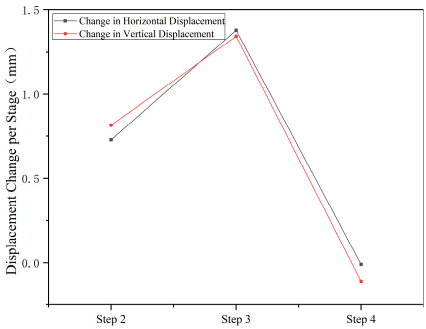

Fig. 8. HSS Model: Change in Tunnel Displacement at Each Stage

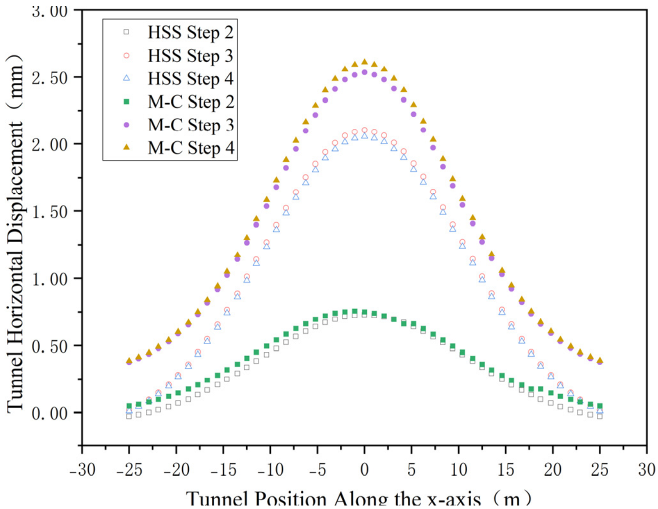

Fig. 9. Horizontal Displacement of Tunnel at Each Stage for Two Models

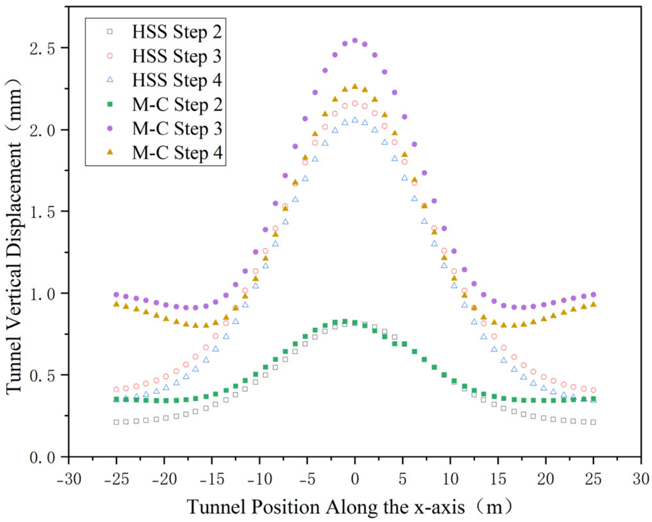

Fig. 10. Vertical Displacement of Tunnel at Each Stage for Two Models

4 Analysis of Different Influencing Factors

As shown in Table 2, three sets of comparative analyses were conducted to study the influence of tunnel distance from the wall (D), diaphragm wall excavation depth (H), and trench segment excavation method on tunnel displacement. Control Group P uses the model described in Section 1, with an excavation depth of 47 m, a tunnel distance of 10 m from the diaphragm wall, and full-face excavation of the 6 m trench segment.

Table 2. Finite Element Analysis Methods and Nomenclature

Variable	Group	Description
Control Group	P	D=10, H=47, 6m segment full-face excavation
Tunnel Distance from Wall	A1	D=8, H=47, 6m segment full-face excavation
	A2	D=12, H=47, 6m segment full-face excavation
Diaphragm Wall Excavation Depth	B1	D=10, H=30, 6m segment full-face excavation
	B2	D=10, H=60, 6m segment full-face excavation
Excavation Method	C	D=10, H=47, 6m segment divided into left and right 3m sections for excavation

4.1 Influence of Horizontal Distance Between Tunnel and Diaphragm Wall

The group A and control group P in figure 11 and 12 from horizontal and vertical displacements we can observe at the point of max displacement where the horizontal separation between the tunnel and the diaphragm wall being 8 meters, 10 meters, and 12 meters this happens at the position most closely associated with the diaphragm wall with the corresponding maximum horizontal displacements 2.54mm, 2.11mm and 1.73mm respectively as well as maximum vertical displacement values 2.27mm, 2.16mm, 2.10mm. So close tunnels get more displacement because they have the closest proximity to the diaphragm wall. As for horizontal and vertical displacement it can be seen that there is an almost opposite link between them and the space which is left between the tunnel and the diaphragm wall.

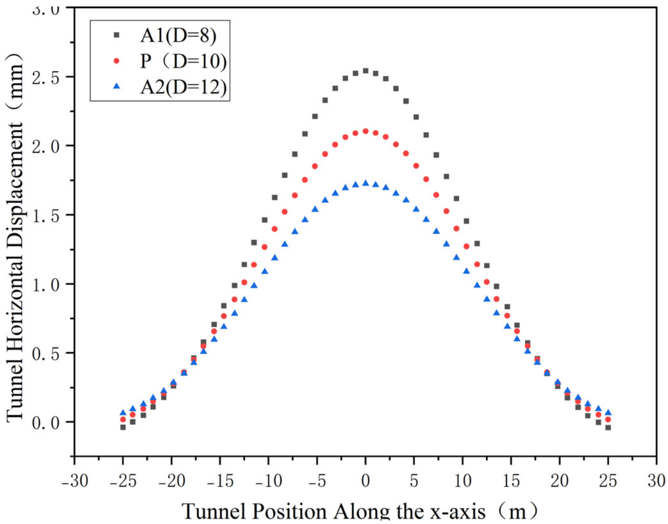

Fig. 11. Tunnel Horizontal Displacement Under Influence of Distance from Wall

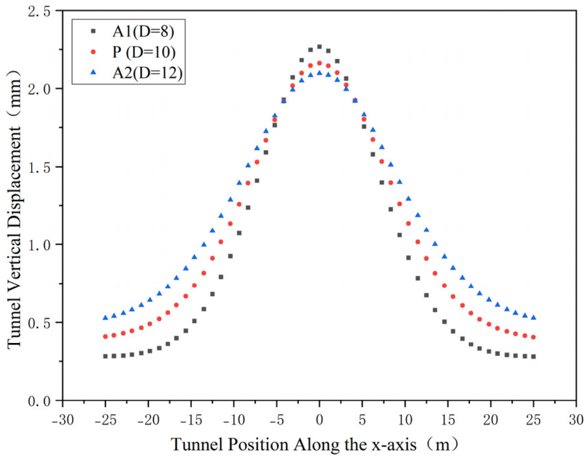

Fig. 12. Tunnel Vertical Displacement Under Influence of Distance from Wall

4.2 Influence of Diaphragm Wall Excavation Depth

As per group b comparing chart of figure 13 and figure 14 it has been noticed that maximum value of x and y displacement will appear nearest to the area which contains location of d w with an excavation of 30m , 47m ,60m. For each case, we have the corresponding maximum horizontal displacements being 1.40mm,2.11mm,2.83mm and the maximum vertical displacements being 1.44mm,2.16mm,2.86mm respectively. This means as the depth of excavation of the diaphragm wall is raised the resulting movement gets even more intense. The tunnel also shows approximate relation to positive correlation on both the horizontal displacement and vertical displacement to the excavation of the diaphragm wall.

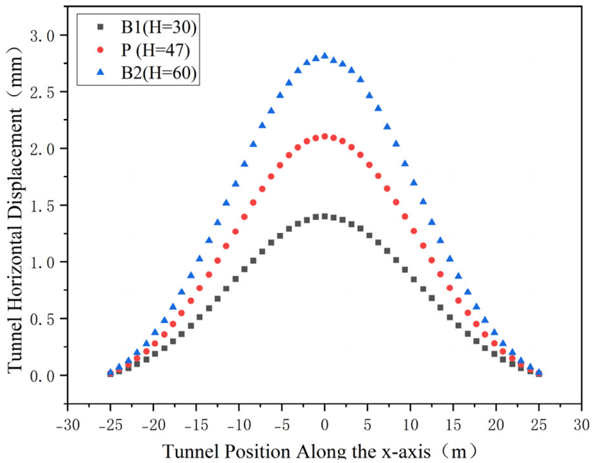

Fig. 13. Tunnel Horizontal Displacement Under Influence of Excavation Depth

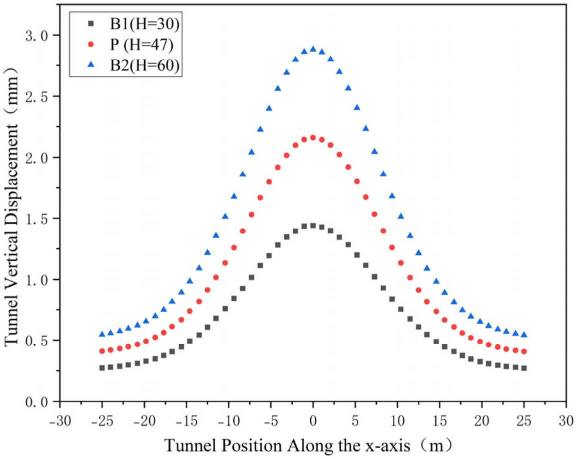

Fig. 14. Tunnel Vertical Displacement Under Influence of Excavation Depth

4.3 Influence of Diaphragm Wall Excavation Method

According to Figure 15 &16 of Group C Horizontal &vertical Displacement Comparison chart we find that if we compare Full face Excavation Vs Two Stage Segment Excavation Trench Segment of Diaphragm wall we found that max Displacement occur at nearest point to diaphragm wall. Corresponding with these max values of horizontal displacement is 2.11mm & 1.26mm; vertical displacements:2.16& 1.29mm. It means we would see lesser induced displacement if we reduce diaphragm wall trench size, since it has same trench size we will get reduced diaphragm wall construction impact on nearby tunnels by having reduced the size of trench.

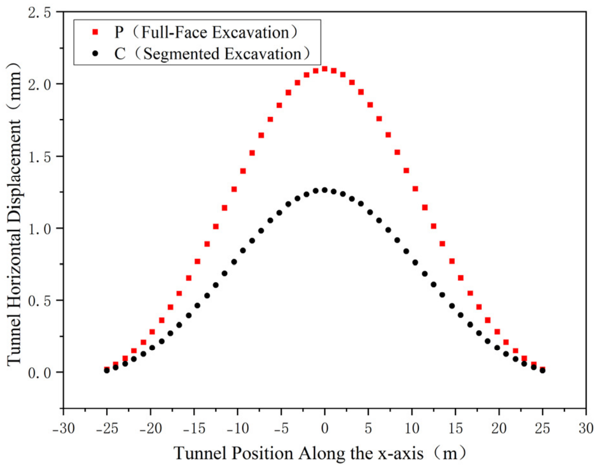

Fig. 15. Tunnel Horizontal Displacement Under Influence of Excavation Method

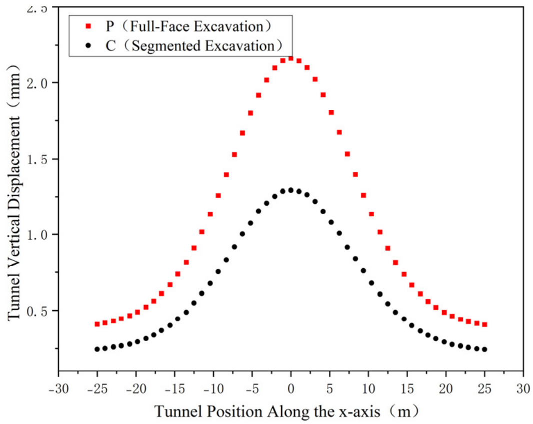

Fig. 16. Tunnel Vertical Displacement Under Influence of Excavation Size/Method

5 Conclusions and Outlook

This paper employs a refined three-dimensional numerical simulation method to systematically investigate the dynamic influence of the phased construction process of diaphragm walls on the deformation of adjacent metro tunnels. A numerical model incorporating four key construction stages—trench excavation, slurry support, concrete pouring, and concrete hardening—is established. By comparing the differences between the HS-Small and Mohr-Coulomb constitutive models, the construction mechanical mechanism, deformation distribution patterns, and key influencing factors are thoroughly analyzed. The main conclusions are as follows:

The influence of diaphragm wall construction on the deformation of adjacent tunnels exhibits distinct stage characteristics. The tunnel displacement induced during the guide wall excavation stage is relatively small. The concrete pouring stage represents the most significant construction phase, during which the horizontal and vertical displacements of the tunnel reach their peak values. This is primarily attributed to the pressure exerted by the fluid concrete on the trench walls, which rapidly replaces the relatively balanced slurry pressure, leading to stress redistribution and release toward the tunnel. The distribution of tunnel displacement along its axial direction can be accurately fitted using a Gaussian distribution function ($R^2 > 0.99$). The maximum displacement occurs at the location closest to the diaphragm wall and decays rapidly with increasing distance, reflecting the spatial disturbance effect. During the concrete hardening stage, a slight rebound in displacement is observed.

The numerical simulation results are highly sensitive to the selection of the constitutive model. Compared with the Mohr-Coulomb model, the HS-Small model, due to its ability to account for the high stiffness at small strains and the loading–unloading path dependency of soils, yields more reasonable and generally smaller predictions of tunnel displacement (particularly vertical heave). Both the horizontal and vertical displacements of the tunnel are negatively correlated with the separation distance. When the separation distance is reduced from 12 m to 8 m, the maximum horizontal displacement increases by approximately 46.8 %, and the maximum vertical displacement increases by approximately 8.1 %. A smaller separation distance dramatically amplifies the influence on the tunnel. Tunnel displacement is positively correlated with the depth of the diaphragm wall. When the excavation depth increases from 30 m to 60 m, the maximum horizontal displacement increases by approximately 102.1 %, and the maximum vertical displacement increases by approximately 98.6 %. Excavation depth is identified as one of the decisive factors controlling tunnel deformation. Compared with the full excavation of a 6 m-wide panel, the "sequential panel excavation" method (first excavating 3 m, then the remaining 3 m) effectively reduces disturbances to adjacent tunnels. This method reduces both the maximum horizontal and maximum vertical displacements by approximately 40.3 %, representing an effective construction optimization measure for deformation control.

(4) It's also important to know that it has no account for groundwater seepage in terms of coupled hydro- mechanical effects at an excavated site. Clayey strata which has much groundwater table generates & dissipates too much excessive pore water stress that can affect the way it moves or changes as well as how tunnel do. And we're still underestimating the sort of time dependent displacement if drainage wasn't that fast. More work should include analysis with flows and deformations together so as to obtain a better picture of transitory hydromechanics and have better estimates of the long term displacements.

References

1. Feng T, Wang Z, Zhang J, et al. A Numerical Simulation Study on the Influence of Foundation Pit Excavation Unloading on Lateral Tunnel:A Metro Station Foundation Pit Excavation in Nanjing as an Example[J]. Journal of East China University of Technology (Natural Science Edition), 2024,47(05):482-494. (in Chinese)
2. Wang P, Zhang L, Yang X, et al. Study on Excavation Method of Foundation Pit of Adjacent and Underlying Existing Shield Metro Line[J]. Modern Tunnelling Technology, 2022,59(S1):396-405. (in Chinese)
3. Mao Z, Ding T, Hu F, et al. The Deformation Characteristics and Patterns of Adjacent Existing Metro Structures Caused by Foundation Pit Excavation Under Different Support Forms[J]. BUILDINGS-BASEL, 2025,15(22):4178.
4. Rui Y, Zhang X, Xue Y, et al. Experimental study of tunnel effects on deformation mitigation in soft clay excavation using centrifuge and PIV[J]. SCI REP-UK, 2025,15(1):29710.
5. Jiang S, Chen W, Ma R, et al. Dynamic Response of Adjacent Tunnels to Deep Foundation Pit Excavation: A Numerical and Monitoring Data-Driven Case Study[J]. Applied Sciences, 2025,15(19):10570.
6. Xu S, Zhou Q, Zheng W, et al. Influences of construction of foundation pits on deformation of adjacent operating tunnels in whole process based on monitoring data [J]. Chinese Journal of Geotechnical Engineering, 2021,43(5):804-812. (in Chinese)
7. Wang T, Li H, Xu R. Analysis of Deformation of Shield Tunnel When Vertical Loading and Unloading[J]. Modern Transportation Technology, 2008(03):29-31. (in Chinese)

8. Zhang S, Feng T, Wang X, et al. Deformation Calculation of Subway-tunnel under Symmetrical Deep Excavation[J]. Science Technology and Engineering, 2016,16(16):263-270. (in Chinese)
9. Yin J. Effects Analysis of Soft Soil Deep Foundation Pit Excavation on Tunnels and Design Parameters Discussion[J]. Chinese Journal of Underground Space and Engineering, 2022,18(S1):173-178. (in Chinese)
10. Wei G. Measurement and analysis of the impact of foundation pit excavation on below existed shield tunnels[J]. Rock and Soil Mechanics, 2013,34(05):1421-1428. (in Chinese)
11. Chen R, Liu S, Meng F, et al. Centrifuge modeling of excavation effects on a nearby tunnel in soft clay[J]. Chinese Journal of Geotechnical Engineering, 2020,42(06):1132-1138. (in Chinese)
12. Chen R, Ashraf A, Meng F. Three-dimensional centrifuge modeling of influence of nearby excavations on existing tunnels and effects of cut-off walls[J]. Chinese Journal of Geotechnical Engineering, 2018,40(S2):6-11. (in Chinese)
13. Clough G, O'Rourke T. Construction induced movements of in situ wall[J]. Geotechnical Special Publication, 1990(25):439-470.
14. Dong Y. Finite element investigation of ground response during diaphragm wall panel installation[J]. CANADIAN GEOTECHNICAL JOURNAL, 2023.
15. Benz T. Small strain stiffness of soils and its numerical consequences[D]. University of Stuttgart, 2006.
16. Wang S, Wang W, Yang H, et al. Study on the Influence of Adjacent Double Deep Foundation Pit Excavation Sequence on Existing Tunnel Deformation Based on HSS Constitutive Model[J]. Applied Sciences, 2024,14(9).
17. Zheng X, Wang X, Shen K, et al. Determination of HSS Model Parameters for Soft Clays in Hangzhou: Statistical Analysis and Engineering Validation[J]. BUILDINGS-BASEL, 2025,15(21):3886.
18. Zhang L, Zhou X, Zhu J. Statistical correlation between HSS model parameters and the method of parameter valuation[J]. IOP Conference Series: Earth and Environmental Science, 2024,1330(1).
19. Lings M, Nash D, Ng C. The lateral pressure of wet concrete in diaphragm wall panels cast under bentonite[J]. Proceedings of the Institution of Civil Engineers: Geotechnical Engineering, 1994,107(3):163-172.
20. Ge P, Zhou A. On selection of common soil constitutive models in numerical simulation of deep foundation pits under complex environment[J]. Journal of Geology, 2020,44(Z1):192-197. (in Chinese)

Open Access This chapter is licensed under the terms of the Creative Commons Attribution-NonCommercial 4.0 International License (http://creativecommons.org/licenses/by-nc/4.0/), which permits any noncommercial use, sharing, adaptation, distribution and reproduction in any medium or format, as long as you give appropriate credit to the original author(s) and the source, provide a link to the Creative Commons license and indicate if changes were made.

The images or other third party material in this chapter are included in the chapter's Creative Commons license, unless indicated otherwise in a credit line to the material. If material is not included in the chapter's Creative Commons license and your intended use is not permitted by statutory regulation or exceeds the permitted use, you will need to obtain permission directly from the copyright holder.